Electronic Supplementary Information for

A 3D porous architecture of Si/Graphene nanocomposite as high-performance anode materials for Li-ion batteries

Xing Xin,[a] Xufeng Zhou,[a] Feng Wang,[b] Xiayin Yao,[a] Xiaoxiong Xu,[a] Yimei Zhu,*[b] and Zhaoping Liu,*[a]

[a] Ningbo Institute of Material Technology and Engineering, Chinese Academy of Sciences,Ningbo, Zhejiang 315201, P.R.China.Fax: +8657486685096; Tel: +8657486685096; E-mail: liuzp@nimte.ac.cn
[b] Condensed Matter Physics and Material Science Department, Brookhaven National Laboratory,Upton, New York, 11973, USA
E-mail: zhu@bnl.gov

Experimental details of GO preparation

6.0 g of KNO_3 and 6.0 g of natural graphite (300 mesh) were added to 270 cm^3 of concentrated H_2SO_4 (98wt.%) at room temperature, and stirred for 10 minutes before slowly adding 36 g of $KMnO_4$ into the mixture. The above mixture was then heated to 40°C and stirred for 6 hrs. Subsequently, under vigorous stirring, 480 cm^3 of water was rapidly added, causing a quick rise in temperature to ~60°C. After, the slurry was continuously stirred at this temperature for another 30 minutes before 1200 cm^3 of water and 36 cm^3 of H_2O_2 solution (30wt.%) were added sequentially to dissolve insoluble manganese species. Finally, the resulting graphite oxide suspension was washed repeatedly in water until the solution pH reached a constant value of ~5.0. The graphite oxide became partially delaminated during washing. We assured the complete delamination of graphite oxide into GO by more mechanical stirring and ultrasonic treatment.

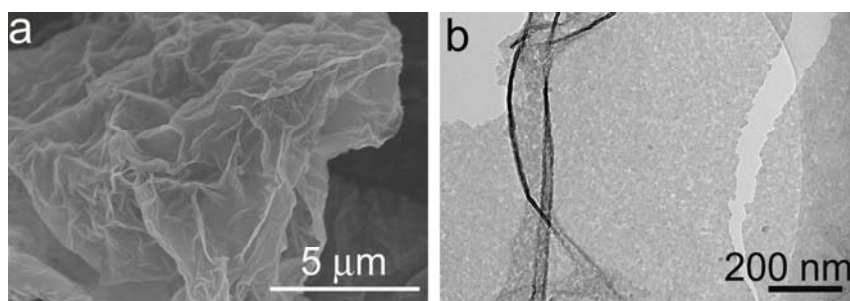**Fig. S1** Digital photographs of the samples prepared at different stages.

Fig. S2 (a) SEM image of the SiO_2@GO nanosheets. (b) TEM image of the calcinated SiO_2@GO nanosheets, which shows thin layers of SiO_2 nanoparticles after removing GO at 600 °C in air.
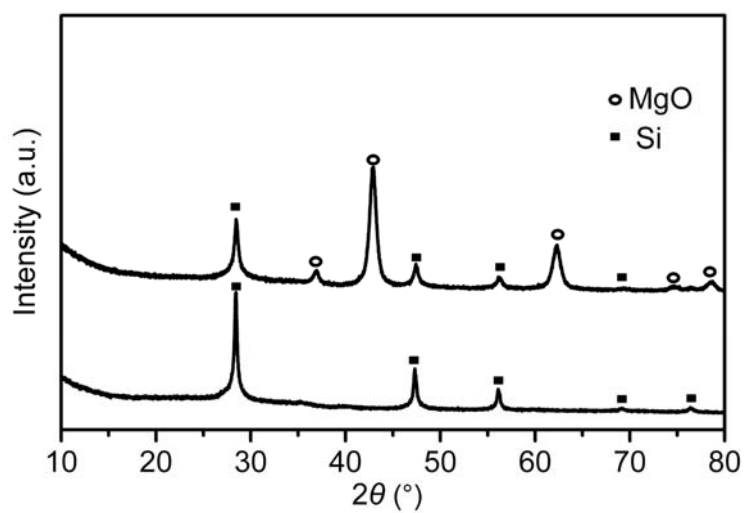

Fig. S3 (a) XRD patterns of (top) the Mg-reduced product and (bottom) the Si@G nanosheets after removing the MgO byproduct.
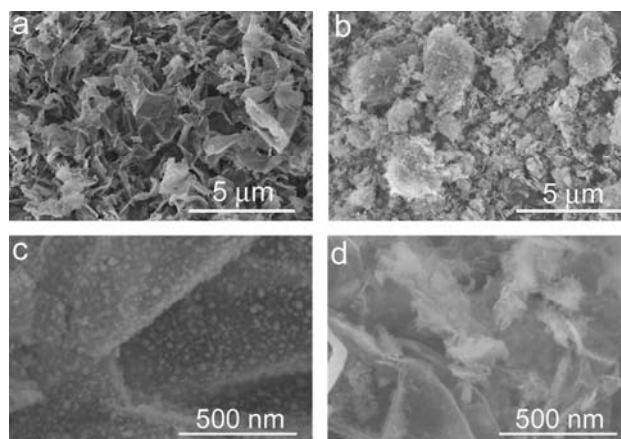
Fig. S4 SEM images of the Si@G nanosheets before (a, c) and after (b, d) HF washing. As can be seen, after removing SiO_x the nanosheets become severe agglomeration and the nanosheets show smooth surfaces without attachment of the Si nanoparticles.
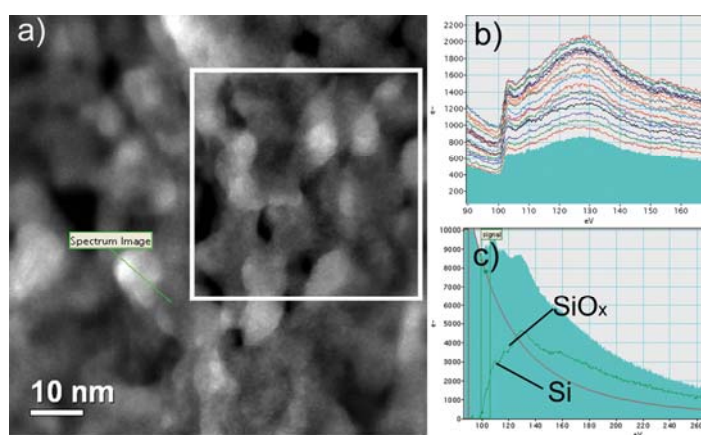

Fig. S5 (a) STEM image showing part of a microsphere, (b) EELS line scan recorded along the green line marked in (a), and (c) Si L23 edge spectrum from the selected area in (a), showing the near-edge fine structure for elemental Si around 110eV, and features at higher energies that may be assigned to SiO_x.
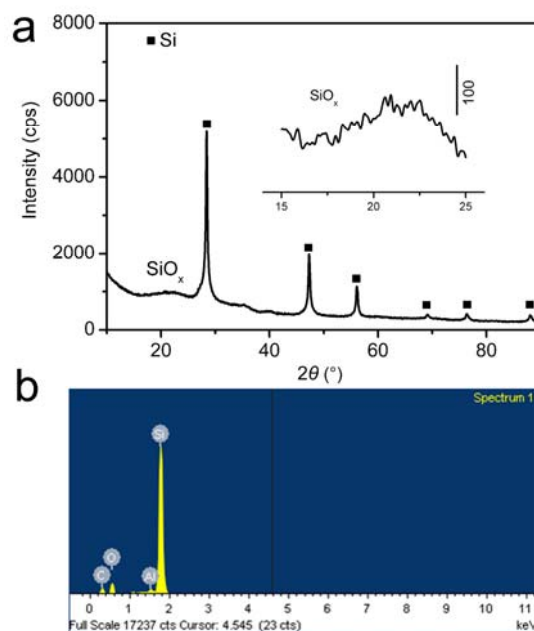

Fig. S6 (a) XRD pattern of the final product, Si/G nanocomposite. The inset is an enlargement of the pattern between 15-25º. (b) Energy dispersive X-ray spectrum (EDS).
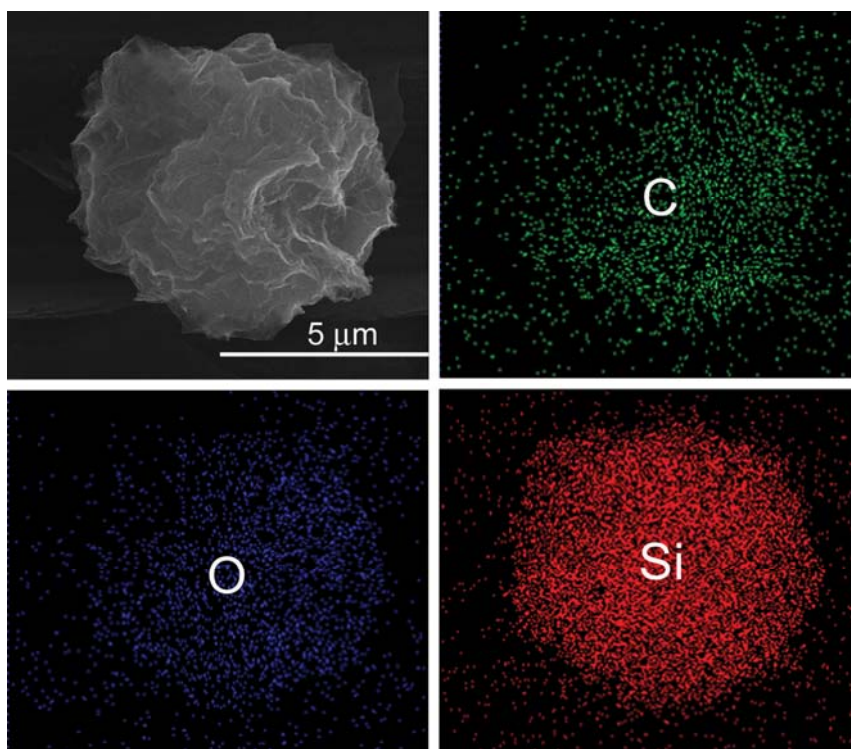
Fig. S7 Elemental maps of carbon, oxygen and silicon of an individual Si/G microsphere.
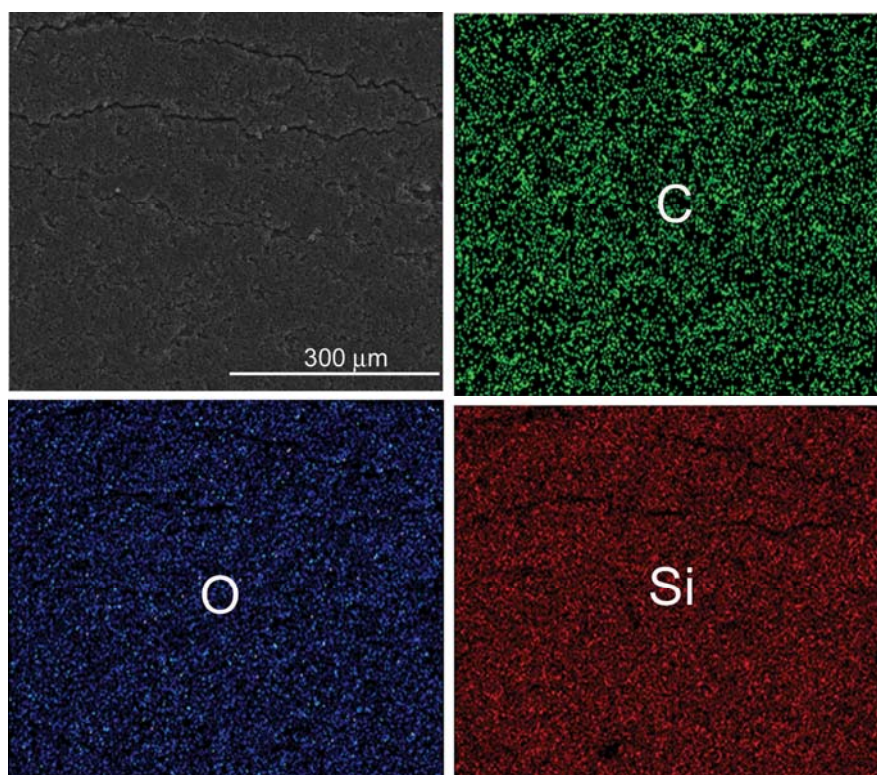

Fig. S8 Elemental maps of the electrode of Si/G nanocomposite after 100 mA g^{-1} to 1 A g^{-1} rate cycles. The electrode maintains the smooth, integrated surface, and the Si, C, O elements distribute homogeneously as the electrode before cycles.
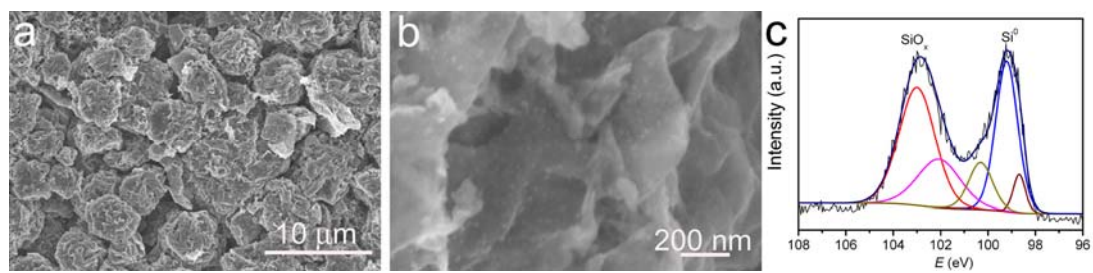
Fig. S9 (a, b) SEM images of the Si/G nanocomposite after 100 mA g^{-1} to 1 A g^{-1} rate cycles. As can be seen, the micro spherical morphology was maintained, and the Si nanocrystals did not fall off from the graphene sheets. (c) XPS spectrum of the Si/G nanocomposite after cycles.